Fingerprint Singular Point Detection Based on Multiple-Scale Orientation Entropy

Hongtao Chen, Liaojun Pang, *Member, IEEE*, Jimin Liang, *Member, IEEE*, Eryun Liu, and Jie Tian, *Fellow, IEEE*

***Abstract*—This letter develops a novel method for fingerprint singular point detection based on a new singularity representation of ridge-valley region called orientation entropy. The candidate singular point is obtained by the multiple-scale analysis of orientation entropy and some post processing steps are proposed to filter the spurious core and delta points. An iteration compensation scheme is proposed to search the precise location for core points against the offset further. Performance of the proposed method has been evaluated on the dataset of FVC2002 DB1. Experimental results show that the multiple-scale orientation entropy is correct and effective for singular detection and the location compensation scheme reduces the distance between the detection result and the truth singular point.**

***Index Terms*—Entropy, multiple-scale analysis, orientation field, orientation field flow curve, singular point detection.**

I. Introduction

FINGERPRINT singular points, core and delta point, are the critical features of fingerprint. The precise singular point location is helpful to image registration, orientation field estimation, fingerprint classification, etc. Many works have been published in literatures for singular detection. They can roughly be classified into three categories: local structure-based, global model-based and filter response-based methods.

The local structure-based methods are mainly based on the tendency of orientation vary according to Poincaré Index (PI) [1]–[4]. In the core, delta and consistent ridge-valley region, the orientation changes differently along a closed circle. They sum these changes of orientation. If the value is $\pm\pi$, there is a singular point; otherwise it is a consistent ridge-valley region. The global model-based methods mainly take the global property of singular point into account to the orientation in the fingerprint [5], [6]. These approaches suppose that the orientation of each ridge-valley region depends on a complex function whose zero and pole points are related to the singular point location. The filter response-based methods detect singular point based on the difference of some especial filter responses between the singular and ridge-valley region [7], [8]. Besides these approaches, there exist other methods [9], [10].

However, the PI-based method is easily affected by noise to detect a considerable number of spurious singular points. It needs additional selection part to filter out these points; the accuracy of the model-based methods depends on the model parameters. Inappropriate parameter selection may cause the failure of fitting method in the singularity region; the filter-based method can either find only one core and delta point or facilitate the more detection to the spurious points.

In this paper, the proposed method gets help from the difference of singularity in fingerprint image areas to develop a new representation for searching the candidate singular point regions. Although the fitting error of model-based methods is eliminated, a slight offset still exists. The compensation scheme, an iteration method based on orientation field flow curve extraction, releases the offset further.

Manuscript received July 12, 2011; revised September 16, 2011; accepted September 18, 2011. Date of publication September 29, 2011; date of current version October 10, 2011. This work was supported by the National Natural Science Foundation of China under Grants 60902083, 60803151, 60875018, 61100234, and 61101247, the Beijing Natural Science Fund under Grant 4091004, and by the Fundamental Research Funds for the Central Universities. The associate editor coordinating the review of this manuscript and approving it for publication was Dr. Saeid Sanei.

H. Chen, L. Pang, J. Liang, and E. Liu are with the School of Life Sciences and Technology, Xidian University, 710071 Xi'an, China (e-mail: htchenGM@gmail.com; pangliaojun@life.xidian.edu.cn; jimleung@mail.xidian.edu.cn; liueryun@life.xidian.edu.cn).

J. Tian is with the School of Life Sciences and Technology, Xidian University, 710071 Xi'an, China and also with the Institute of Automation, Chinese Academy of Sciences, 100190 Beijing, China (e-mail: tian@life.xidian.edu.cn; tian@ieee.org).

Color versions of one or more of the figures in this paper are available online at http://ieeexplore.ieee.org.

Digital Object Identifier 10.1109/LSP.2011.2169957

II. Multiple-Scale Orientation Entropy

A. Orientation Extraction

A gradient-based method for smooth orientation extraction [11] is used to estimate the pixel-wise orientation image $I_o(o \in [0, \pi))$. This method applied three different scale Gaussian filters to achieve the smooth orientation without excessive runtime. The detail is summarized as follows.

Let I refer to the fingerprint image and $g = \{g_i | g(\sigma_i, \omega_i), i = 1, 2, 3\}$ denote to three isotropic Gaussian filters with the block size ω_i, the pixel-wise squared gradient vector is

$$\begin{bmatrix} G_{gs,x} \\ G_{gs,y} \end{bmatrix} = \begin{bmatrix} G_{gx}^2 - G_{gy}^2 \\ 2G_{gxy} \end{bmatrix} = g_2 * \begin{bmatrix} G_x^2 - G_y^2 \\ 2G_{xy} \end{bmatrix} \tag{1}$$

where $G_x^2 = G_x \cdot G_x$, $G_y^2 = G_y \cdot G_y$, $G_{xy} = G_x \cdot G_y$ and the gradient vector $[G_x, G_y]^T$ is

$$\begin{bmatrix} G_x \\ G_y \end{bmatrix} = \begin{bmatrix} (\partial g_1/\partial x) * I \\ (\partial g_1/\partial y) * I \end{bmatrix}. \tag{2}$$

The smooth orientation o is computed by

$$o = \frac{1}{2}\tan^{-1}\left(\frac{g_3 * \sin(\phi)}{g_3 * \cos(\phi)}\right) + \pi/2 \tag{3}$$

where $\sin(\phi)$ and $\cos(\phi)$ is derived from (4) by

$$\begin{aligned} \sin(\phi) &= G_{gs,y}/\sqrt{G_{gs,x}^2 + G_{gs,y}^2} \\ \cos(\phi) &= G_{gs,x}/\sqrt{G_{gs,x}^2 + G_{gs,y}^2} \end{aligned} \tag{4}$$

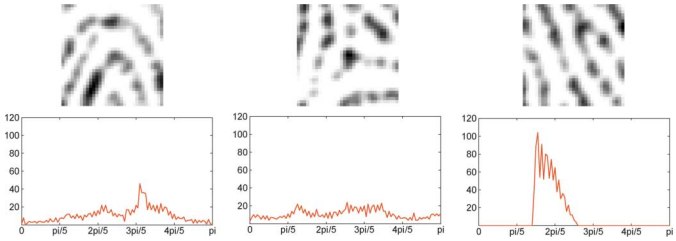

Fig. 1. Orientation distribution of different regions. The first row is the different regions and the second row is the corresponding orientation distribution. The first column is for core point region. The second column is for delta point region. The third column is for consistent ridge-valley region.

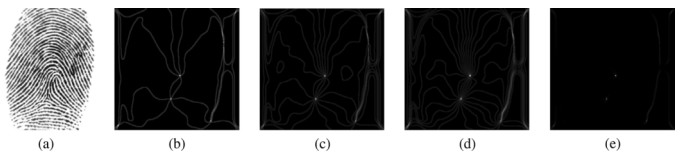

Fig. 2. Example of MSOE. (a) Original image; (b) π/n_1 scale orientation entropy; (c) π/n_2 scale orientation entropy; and (d) π/n_3 scale orientation entropy;(e). Multiple-scale orientation entropy. n_1, n_2 and n_3 are the different sampling rates.

B. Orientation Entropy

In information theory, entropy is a description to the uncertainty of a random variable. In Fig. 1, the histograms of orientation in different fingerprint regions are shown. The orientation has more evenly distribution in the singular region than consistent ridge-valley region. Here, we apply Shannon's definition [12] to the discrete entropy to obtain the orientation entropy (OE).

Suppose the orientation field o is a random variable. π/n is the quantification scale and used to quantify o as discrete variable θ with possible values $(\theta_1, \theta_2, \ldots, \theta_n)$. The discrete orientation θ can be computed according to (5)

$$\theta = \frac{\pi}{n}\left(\frac{o}{\pi/n} \bmod n\right),\ n = 2, 3, 4, \ldots \tag{5}$$

where n is the sample rate of the orientation field.

Let $I_{b\theta}$ be the quantified orientation image in a block size B. The discrete entropy $H^n_{b\theta}$ of $I_{b\theta}$ is

$$H^n_{b\theta} = -\sum_{i=1}^{n} p(\theta_i)\log_{10} p(\theta_i) \tag{6}$$

where p is the distribution of the probability mass function.

C. Multiple-Scale Analysis

However the quantification releases the computation complexity of orientation entropy, many noise regions are strengthened in the single quantification scale case. Multiple-scale analysis is helpful to reduce the effect from the region where the orientation is around the possible value.

Let $\pi/n_1, \pi/n_2$ and π/n_3 be three different scales to quantify the orientation. The multiple-scale orientation entropy (MSOE) is defined as follows:

$$H_{MSb\theta} = H^{n_1}_{b\theta} H^{n_2}_{b\theta} H^{n_3}_{b\theta}. \tag{7}$$

Fig. 2 shows an example of OE using three different scales and MSOE.

III. Candidate Singular Detection

From the Fig. 2, we can find that the MSOE feature has a significant difference between in the singularity region and in the smooth ridge-valley region. The global and local thresholds [13] are used to select the candidate singular point region in the foreground region which is extracted by the method [14].

Let $H_{MSb\theta}(i,j)$ be the MSOE at pixel (i,j). The candidate singular point is decided by T_g and $T_{lmax}(i,j)$. If $H_{MSb\theta}(i,j) > T_g, H_{MSb\theta}(i,j) = T_{lmax}(i,j)$, the pixel (i,j) is a candidate singular point, where $T_g = C\prod_{i=1}^{3}(1/n_i)\log_{10}(1/n_i)$ and $T_{lmax}(i,j)$ is a local maximum value, which can be estimated adaptively in the block size w_l as follows:

$$T_{lmax}(i,j) = \arg\max_{i,j}\left\{H_{MSb\theta}(i+u, j+v)\right\},\quad u, v \in [-w_l/2, w_l/2). \tag{8}$$

C is a constant coefficient. The singular type is confirmed by the conventional PI method.

Although the smooth orientation field reduces the effect from noise and the threshold scheme filters out a lot of spurious points, some regions around singular point are detected. To distinguish the truth singular points from the spurious ones in the candidate set S, the post processing steps are applied as below.

If a core point is too closed (16 pixels) to a delta point, they are removed from S; If there are more than one core point in S, the core point with maximum OE (cp_{moe}) and all the points with similar singular direction [2] are kept in the set S_{cm}, and all the points with contrary direction are kept in the set S_{cmc}. Let o_{moe} be the direction of cp_{moe}, the elements in S_{cm} and S_{cmc} are projected along o_{moe} and $\pi + o_{moe}$. Except the points with maximum projection value in the two sets, all other core points are removed from S; For the region B_d around each delta point in S, the orientation entropy is extracted with $\pi/3$ as quantification scale. If more than three connectivity regions with zero value in B_d exist and the area difference between the regions with maximum area and the third maximum area is not too much, the point is a valid delta point, otherwise it is removed from S.

IV. Compensation Scheme Based on Orientation Field Flow Curve

Smooth orientation leads to a slight offset of the core point location. In addition, the nonuniform orientation changes around the core point have the similar effect.

A novel algorithm based on orientation field flow curves (OFFCs) is proposed to compensate the offset. Here, the coarse orientation [2] is used to extract the OFFCs. The compensation algorithm for each candidate core point region is described as follows.

Step 1) The initial iteration time τ is set to 1 and the candidate core point is set as the initial start point for the extraction of the first OFFC.

Step 2) The τth OFFC $l^\tau = \{p^\tau_i\}_{i=1}^{J_\tau}$ is iteratively extracted from the initial start point sp^τ of l^τ according the method in [15], where J_τ is the length of l^τ.

Step 3) Estimate the maximum curvature point p^τ_{mc} on l^τ and the reference direction. Let p^τ_{i-2d}, p^τ_{i-d}, p^τ_i, p^τ_{i+d}

TABLE I
PARAMETER VALUES

Parameter(s)	Description	Value
B	Block size for orientation entropy	4
(n_1, n_2, n_3)	Three scale for MSOE	(6,12,18)
C	Coefficient of global threshold	0.16
w_l	Block size of local threshold	32
d	step for flow extraction	2
τ_{max}	Max iteration number	3
d_c	Offset step	9

and p^{τ}_{i+2d} be the points on l^{τ} with the sample step d, the curvature ω on p^{τ}_i is computed according to the cosine theorem as

$$\begin{aligned}\omega_{p^{\tau}_i} &= 1 - \cos\alpha_{p^{\tau}_i} \\ &= 1 - \frac{2d^2 - \left|\overrightarrow{p^{\tau}_{i-d}p^{\tau}_{i+d}}\right|^2}{2d^2} \\ &= \frac{\left|\overrightarrow{p^{\tau}_{i-d}p^{\tau}_{i+d}}\right|^2}{2d^2}. \end{aligned} \tag{9}$$

The reference direction is obtained by the location of p^{τ}_{mc} and p_r on l^{τ}

$$\theta_r = arg(\overrightarrow{p^{\tau}_{mc}p_r}) \tag{10}$$

where the location of p_r is the mean location of the four sample points p^{τ}_{k-2d}, p^{τ}_{k-d}, p^{τ}_{k+d} and p^{τ}_{k+2d}, k is the label of p^{τ}_{mc}.

Step 4) Find the initial start point for the next OFFC $l^{\tau+1}$. Suppose d_c is the offset step, the initial start point of $l^{\tau+1}$ is

$$sp^{\tau+1} = p^{\tau}_{mc} + d_c(\cos\theta_r, \sin\theta_r). \tag{11}$$

Step 5) If $\tau = \tau_{max}$, the core point p_c is the point with maximum curvature in $\{p^i_{mc}\}^{\tau_{max}}_{i=1}$. Otherwise $\tau = \tau + 1$ and go to Step 2) to extract $l^{\tau+1}$.

The OFFC extraction is within the effective region centered at its initial start point. It ensures that there can be only one core point in the region for compensation.

V. EXPERIMENTAL RESULTS

We compare the performance of singular detection on the public fingerprint database FVC2002 DB1 [16] with another two methods [1], [8], where all the detection algorithms are based on the smooth orientation [11]. The DB1 from FVC2002 contains 800 fingerprints and the scanning resolutions are 500 DPI. All the truth singular points in the fingerprint database are manually labeled. The truth and detected singular points are considered as the correspondence pair if their distance is smaller than 30 pixels. The parameters of our method corresponding to the database are given in the Table I. For the conventional PI method, the average core (or delta) point is computed to replace these core (or delta) points in a small region.

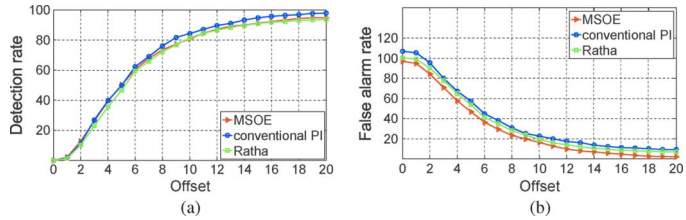

Fig. 3. (a) Relationship between offset and detection rate for MSOE and (b) relationship between offset and false alarm rate for MSOE.

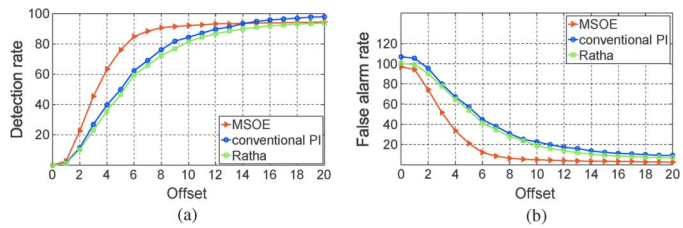

Fig. 4. (a) Relationship between offset and detection rate for compensation scheme to MSOE and (b) relationship between offset and false alarm rate for compensation scheme to MSOE.

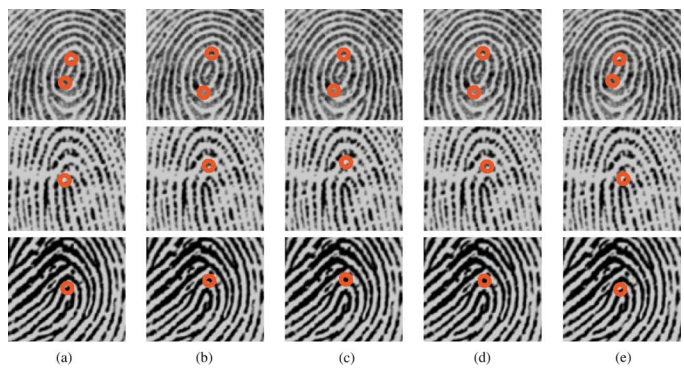

Fig. 5. Example of the compensation results. (a) manual, (b) conventional PI method, (c) Chikkerur's method, (d) MSOE, and (e) compensation scheme for MSOE.

To evaluate the effectiveness of MSOE, the relationship between offset and detection rate and the relationship between offset and false rate are plotted in Fig. 3. It shows that the method only based on MSOE has lower false alarm rate than the two other methods meanwhile it has similar detection rate as the two other methods.

The relationship between the offset and detection rate for compensation scheme and two other methods are plotted in Fig. 4(a). There are more match pairs of truly detected singular point and truth singular point with the small offset. Accomplishing the offset correction, the false alarm rate is further reduced [see Fig. 4(b)].

In Fig. 5, the core point region is only given. The experimental results show that the compensation scheme can effectively amend the offset. Combing the multiple-scale analysis to the orientation entropy and the compensation scheme, the proposed method provides a good performance for singular detection (see Fig. 6).

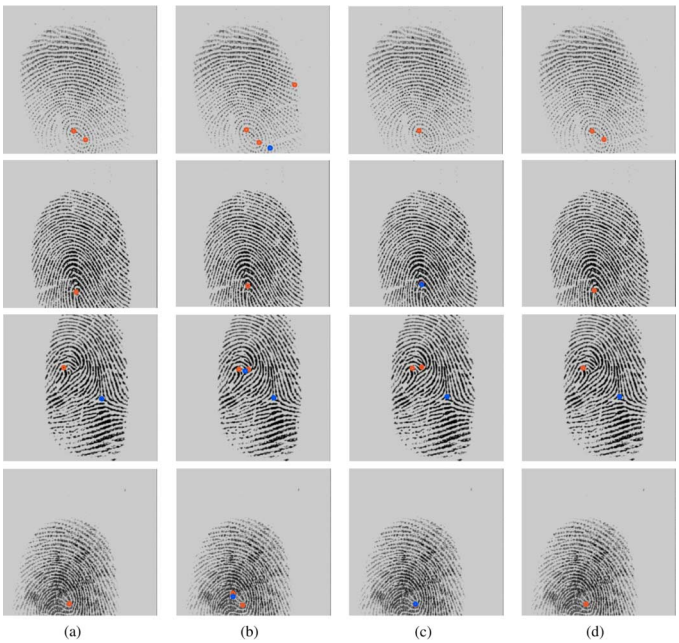

Fig. 6. Some examples of the final detection results. (a) Manual, (b) conventional PI method, (c) Chikkerur's method, and (d) the proposed method.

VI. Conclusion

By analyzing the orientation field distribution, we have proposed a method to extract the fingerprint singular point based on MSOE. The preliminary results on the public database of FVC2002 DB1 indicate that the new feature is recognizable for the orientation field singularity and the compensation scheme reduces the offset between the truly detected core point and the corresponding truth core point successfully.

However, the further experiments on the database with the bad image quality are still needed. The singular point type and direction may be confirmed according to the MSOE. The proposed singular detection method may be helpful for improving the fingerprint match performance of the free alignment technology [17], [18].

References

[1] D. Maltoni, D. Maio, A. K. Jain, and S. Probhaker, *Handbook of Fingerprint Recognition*. New York: Springer-Verlag, 2008.
[2] A. M. Bazen and S. H. Gerez, "Systematic methods for the computation of the directional fields and singular points of fingerprints," *IEEE Trans. Patt. Anal. Mach. Intell.*, vol. 24, no. 7, pp. 905–919, Jul. 2002.
[3] C. L. Jin and H. Kim, "Pixel-level singular point detection from multi-scale Gaussian filtered orientation field," *Patt. Recognit.*, vol. 43, no. 11, pp. 3879–3890, Nov. 2010.
[4] J. Zhou, F. L. Chen, and J. W. Gu, "A novel algorithm for detecting singular points from fingerprint images," *IEEE Trans. Patt. Anal. Mach. Intell.*, vol. 31, no. 7, pp. 1239–1250, Jul. 2009.
[5] B. Sherlock and D. Monro, "A model for interpreting fingerprint topology," *Patt. Recognit.*, vol. 26, no. 7, pp. 1047–1055, 1993.
[6] L. Fan, S. Wang, H. Wang, and T. Guo, "Singular points detection based on zero-pole model in fingerprint image," *IEEE Trans. Patt. Anal. Mach. Intell.*, vol. 30, no. 6, pp. 929–940, 2008.
[7] J. Bigun, T. Bigun, and K. Nilsson, "Recognition by symmetry derivatives and the generalized structure tensor," *IEEE Trans. Patt. Anal. Mach. Intell.*, vol. 26, no. 12, pp. 1590–1605, Dec. 2004.
[8] S. Chikkerur and N. Ratha, "Impact of singular point detection on fingerprint matching performance," in *IEEE Workshop on Automatic Identification Advanced Technologies*, 2005, pp. 207–212.
[9] G. Cao, Z. H. Mao, and Q. S. Sun, "Core-point detection based on edge maps in fingerprint images," *J. Electron. Imag.*, vol. 18, no. 1, 2009.
[10] A. Ahmadyfard and M. S. Nosrati, "A novel approach for fingerprint singular points detection using 2D-wavelet," in *IEEE/ACS Int. Conf. Computer Systems and Applications*, May 13–16, 2007, pp. 688–691.
[11] C. Jin and H. Kim, "High-resolution orientation field estimation based on multi-scale Gaussian filter," *IEICE Electron. Exp.*, vol. 6, no. 24, pp. 1781–1787, Dec. 2009.
[12] C. E. Shannon, "A mathematical theory of communication," *Bell Syst. Tech. J.*, vol. 27, pp. 379–423, July and Oct. 1948, and 623–656.
[13] R. C. Gonzalez and R. E. Woods, *Digital Image Processing*. Englewood Cliffs, NJ: Prentice-Hall, 2002.
[14] A. Baig, A. Bouridane, and F. Kurugollu, "A corner strength based fingerprint segmentation algorithm with dynamic thresholding," in *Int. Conf. Pattern Recognition*, Dec. 8–11, 2008, pp. 1–4.
[15] S. C. Dass and A. K. Jain, "Fingerprint classification using orientation field flow curves," in *Proc. CVGIP*, 2004, pp. 650–655.
[16] FVC2002 [Online]. Available: http://bias.csr.unibo.it/fvc2002/ 2002
[17] H. Chen, J. Tian, and X. Yang, "Fingerprint matching with registration pattern inspection," in *Proceedings of the 4th Int. Conf. Audio-and Video-Based Biometric Person Authentication*, Jun. 2003, pp. 327–334.
[18] X. J. Chen, J. Tian, and X. Yang, "An algorithm for distorted fingerprint matching based on local triangle features set," *IEEE Trans. Inf. Forensics Secur.*, vol. 1, no. 2, pp. 169–177, June 2006.